Renewable Energy 99 (2016) 289–294

Contents lists available at ScienceDirect

Renewable Energy

journal homepage: www.elsevier.com/locate/renene

Polyaniline-wrapping hollow sulfur with MCM-41 template and improved capacity and cycling performance of lithium sulfur batteries

Yan ling An [a], Wenlong Song [a, b, **], Pan Wei [a], Meiqiang Fan [a, b, *], Haichao Chen [a], QiangJian Ju [a], Da Chen [a], Guanglei Tian [a], ChunJu Lv [a], Kangying Shu [a]

[a] Department of Materials Science and Engineering, China Jiliang University, Hangzhou 310018, PR China
[b] Zhejiang Tianneng Energy Technology Co., Ltd., Changxing County, Zhejiang Province 313100, PR China

ARTICLE INFO

Article history:
Received 1 April 2016
Received in revised form
11 June 2016
Accepted 30 June 2016

Keywords:
Lithium/sulfur battery
Polyaniline wrapping hollow sulfur composite
Conductive polymer
MCM-41

ABSTRACTS

A conductive polyaniline-wrapping hollow sulfur composite used as a cathode material for lithium/sulfur batteries was successfully fabricated by a facile and controllable chemical reaction with MCM-41 template. The polyaniline-wrapping hollow sulfur composite had a good reversible capacity of 506.3 mAh g^{-1} at the 150th cycle, reflecting the low loss of sulfur and polysulfide encapsulated by polyaniline during the charge and discharge cycles. The results of SEM and EIS show that the polyaniline-wrapping hollow sulfur composite presented many good electron-conducting paths for the rechargeability of lithium/sulfur battery. XRD and TG-DSC results revealed the formation of fine sulfur particles encapsulated by polyaniline and sulfur distributed on the polyaniline surface because of low sulfur melting temperature, which was the key reason for the activation.

1. Introduction

Energy storage is a key factor related to sustainable development worldwide. Lithium ion battery is a new and attractive green energy storage device, which has developed rapidly over the last decade. This battery is a good choice for mobile phones, notebook computers, portable electric tools, and electric vehicles because it possesses high specific capacity, long cycle, and no environmental pollution, among others. However, conventional lithium ion battery still has low energy density and high cost, which prevent wide application in electric vehicles. It is the key factor to develop high-performance and low-cost materials and fabrication technologies for lithium ion battery. Compared with the other components of lithium ion battery, the cathode electrode material is the key component that affects electrochemical performance, safety, and cost of the entire cell. $LiFePO_4$, $LiCoO_2$, and $LiMn_2O_4$ are widely used cathode materials for commercial lithium ion battery. These cathode materials have low theoretical capacity and cannot meet the growing energy density requirement of batteries. Sulfur-based materials are a promising cathode; sulfur has many advantages, such as high theoretical capacity (1672 mAh g^{-1}), low cost and abundant reserves [1–3], compared to conventional lithium-ion batteries and other emerging lithium-based batteries. However, several difficulties exist for sulfur application in lithium ion batteries because sulfur has an insulating nature, large volume expansion, and dissoluble polysulfide species formed in the discharge process [4,5]. These shortcomings lead to capacity fading, Coulombic efficiency decrease, and low C-rate because of the loss of active materials and the side reactions on the lithium metal anode. Resolving these shortcomings is necessary to stimulate the development of sulfur cathode.

Sulfur particles limited inside the conductive polymers is a good method for improving the electrochemical performance of sulfur cathode. A polymer presents a flexible nanostructure and contains a large void space inside the polymer shell, which can accommodate the volume expansion of sulfur and decrease polysulfide dissolution during lithiation [6]. The sulfur cathode coated or modified with electro-polymerized conductive polyaniline (PANI) and polyprrole had improved the electrochemical performance of rechargeable batteries [7,8]. Qiu [9] co-heated the mixture of pyrrole-co-aniline (PPyA) and sublimed sulfur at 160 °C for 24 h, where the sulfur was limited inside the nanofiber network

* Corresponding author. Department of Materials Science and Engineering, China Jiliang University, Hangzhou 310018, PR China.
** Corresponding author. Department of Materials Science and Engineering, China Jiliang University, Hangzhou 310018, PR China.
E-mail address: fanmeiqiang@126.com (M. Fan).

http://dx.doi.org/10.1016/j.renene.2016.06.062
0960-1481/

structure of PPyA. The nano-dispersed composite exhibited an initial specific capacity of up to 1285 mAh g^{-1} and remained at 866 mAh g^{-1} after 40 cycles. Xiao L. prepared a vulcanized polyaniline nanotube/sulfur composite by heating a mixture of polyaniline nanotube and sulfur at 280 °C. The composite presented a discharge capacity of 837 mAh g^{-1} after 100 cycles at 0.1 C [10]. The improved electrochemical performance of the composite was due to the fine sulfur encapsulated in polyaniline, which provided a self-breathing and flexible framework and reduced stress and structure degradation. However, uniform mixing of sulfur and polymer needs high heating temperature and long co-heating time, which may damage the polymer structure.

In this study, a polyaniline-wrapping hollow sulfur composite was designed and prepared through chemical reaction at room temperature with MCM-41 (silica) as template. The sulfur deposition amount and rate on MCM-41 surface could be regulated by the reaction of $Na_2S_2O_8$ and hydrochloric acid (HCl). PANI was deposited on the particle surface through chemical oxidative polymerization [11,12]. The nano-structure of fine hollow sulfur encapsulated in polyaniline can provide many electron-conducting paths and thereby improve electrochemical performance.

2. Experimental methods

2.1. Preparation of PANI-wrapping hollow sulfur

Polyaniline-wrapping hollow sulfur composite was prepared though a three-step process. First, 0.1 g of MCM-41 99 wt% (Nan Jing Xinfeng, China), 0.091 g of cetyltrimethyl ammonium bromide (CTAB, analytical reagent), and 4.74 g of $Na_2S_2O_3$ (analytical reagent) were added to 250 ml of deionized water, and the mixture was stirred for 5 h. Thereafter, 100 ml of diluted HCl (mass fraction of 2%) was added dropwise to the mixture, which was stirred continuously at room temperature. Sulfur was successively deposited on the MCM-41 surface through the reaction of $Na_2S_2O_3$ and HCl in the following equation:

$$2HCl + Na_2S_2O_3 = 2NaCl + H_2O + S\downarrow + SO_2\uparrow \quad (1)$$

First, the mixture was filtered and dried to obtain S/MCM-41 composite. Second, the obtained S/MCM-41 composite, 0.091 g of CTAB, and 0.2 ml of An were added to 200 ml of diluted HCl (mass fraction of 3.5%) and sonicated for 1 h. Approximately 1 g of $Na_2S_2O_8$ (AR) was added dropwise to the mixture and stored at 0 °C with constant magnetic stirring for 3 h. The mixture was then filtered and dried to obtain the polyaniline-wrapping S/MCM-41 composite. Lastly, the polyaniline-wrapping S/MCM-41 composite was added to the HF solution and stored for 24 h. The polyaniline-wrapping hollow sulfur composite was acquired after filtration, cleaning, and drying. The detailed synthesis of the polyaniline-wrapping hollow sulfur composite is described in Fig. 1. Separate sulfur and PANI were synthesized for comparison at similar conditions.

2.2. Microstructure characterization

Powder X-ray diffraction (XRD) patterns of the polyaniline-wrapping hollow sulfur composite were performed on an X-ray diffractometer (RIGAKU, Japan, model D/MAX2550V/PC). Surface morphology tests were carried out using a scanning electron microscope (JSM-5610LV) attached with EDS and transmission electron microscope (JEOL JEM-2100). The sulfur content in the polyaniline-wrapping hollow sulfur composite was collected using thermogravimetric analysis (METTLER Toledo SMP/PF7548) at argon atmosphere, with a temperature increase rate of 10 °C/min.

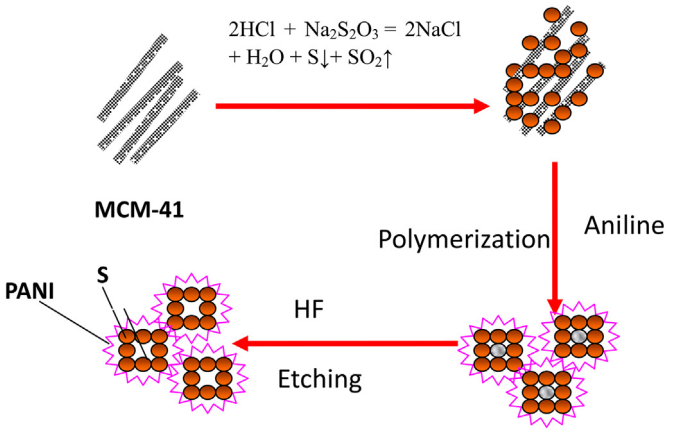

Fig. 1. Microstructure evolution of polyaniline-wrapping hollow sulfur composite in preparation process.

2.3. Electrochemical measurements

CR2025-type coin cells were fabricated with sulfur and polyaniline-wrapping hollow sulfur composite as the cathode and lithium as the anode. The detailed electrode preparation technology and assembly process were introduced in our previous work [13]. Cathode (80 wt%), acetylene black (10 wt%), and polyvinylidene fluoride binder (10 wt%) were mixed in *N*-methylpyrrolidinone solvent, and the mixture was stirred for 10 h at room temperature. The mixture was then uniformly scribbled on the surface of an aluminum foil and dried at 60 °C under vacuum for 10 h. The coin cell was assembled in an Ar-filled glove box and was used for electrochemical characterization. In this study, 1 M bis(-trifluoromethane) sulfonamide lithium salt (Sigma Aldrich) and 0.1 M $LiNO_3$ in a mixture of 1,3-dioxolane and 1,2-dimethoxyethane (volume ratio of 1:1) were used as the electrolyte.

The galvanostatic charge/discharge performance tests of the sulfur cathode were performed within the potential range of 1.5 V–3.0 V by using a LAND CT2001A battery-testing system at room temperature. All cells were discharged to 1.5 V before the test started. Specific capacities and charge/discharge current densities were calculated based on the sulfur weight in the cathode. Cyclic voltammetry (CV) and electrochemical impedance spectroscopy (EIS) were performed in the CHI660E electrochemical

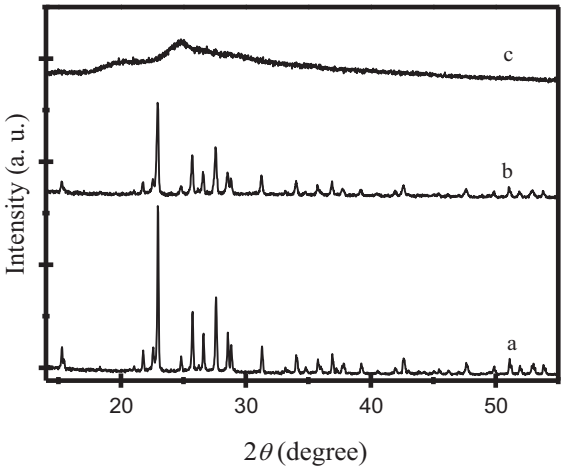

Fig. 2. XRD patterns of the sulfur (a), polyaniline wrapping hollow sulfur composite (b) and PANI(c).

measurement system. CV tests were conducted with a voltage range of 1.5 V–3.0 V versus Li^+/Li at a scanning rate of 0.2 mV s^{-1}. EIS was determined within the frequency range of 100 kHz to 0.01 Hz with an AC voltage amplitude of 5 mV at open-circuit voltage.

3. Results and discussion

3.1. Microstructure characteristics

Fig. 2 shows XRD patterns of PANI, sulfur, and polyaniline-wrapping hollow sulfur composite. All peaks corresponding to sulfur (JCPDS: 08-0247) were identified in the XRD patterns of sulfur and polyaniline-wrapping hollow sulfur composite, as a wide peak corresponding to an amorphous phase was observed in the XRD patterns of PANI. The sulfur peak lines of the polyaniline-wrapping hollow sulfur composite were slightly wider than those of the sulfur particle, indicating that the hollow sulfur particles wrapped by polyaniline have a smaller grain size than those of sulfur.

The detailed morphologies of sulfur, MCM-41, S/MCM-41, and polyaniline-wrapping hollow sulfur composite were collected and shown in Fig. 3. The sulfur particles are flat with irregular shapes, and the sulfur particle size ranges from several micrometers to tens of micrometers, as shown in Fig. 3a. The MCM-41 exhibited nanofibers with several micrometers in length and tens of nanometers

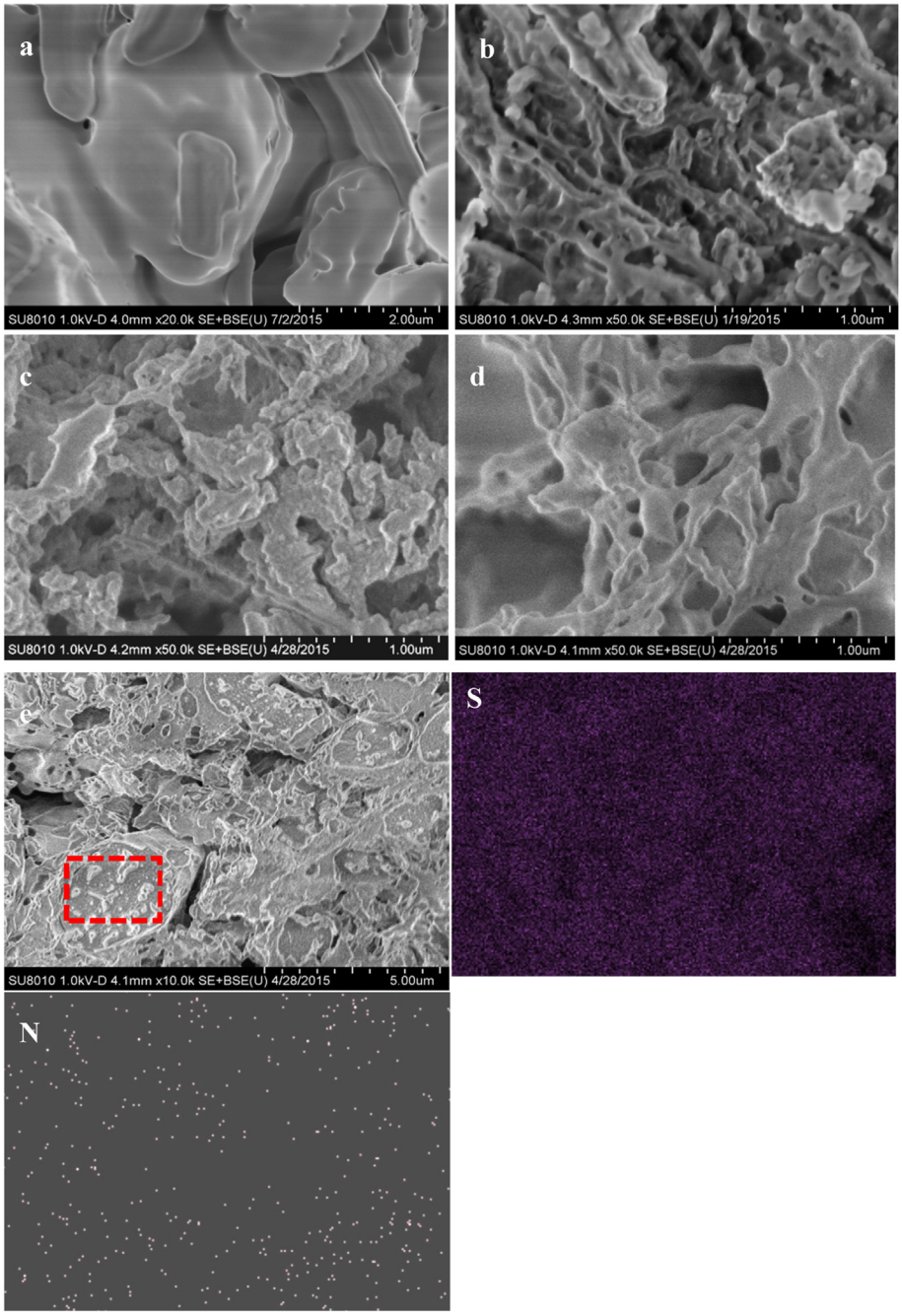

Fig. 3. SEM images of the sulfur (a), MCM-41 (b), S/MCM-41 (c), polyaniline wrapping hollow sulfur composite (d, e) and EDS mapping in polyaniline wrapping hollow sulfur composite (e).

in width and presented a hollow network structure (Fig. 3b). After sulfur was deposited on the MCM-41 surface, the flat sulfur particles with several hundreds of nanometers in diameter were observed (Fig. 3c). The existence of MCM-41 prevented the agglomeration of sulfur particles and regulated the particle size of sulfur in the preparation process. Thin nanofibers of PANI coating sulfur and numerous pores were observed (Fig. 3d and e) after MCM-41 was etched in the HF solution, indicating that polyaniline wrapped the surface of the hollow sulfur. The distribution of PANI and sulfur is presented in Fig. 3e, where element N was uniformly distributed around element S. The results confirmed that PANI was uniformly coated on the sulfur surface. For further observation, transmission electron microscopy (TEM) was performed to characterize the nanostructure of the polyaniline that wrapped the surface of the hollow sulfur composite. Many tens of nanometers of PANI nanofibers were observed on the sulfur surface, as shown in Fig. 4a and 4b, showing that fine hollow sulfur was encapsulated by amorphous PANI.

Fig. 5 shows the TG-DSC of sulfur, PANI, and polyaniline-wrapping hollow sulfur composite. Sulfur began to lose weight at 200 °C and lost approximately 100 wt% before reaching 320 °C (Fig. 5a). The polyaniline-wrapping hollow sulfur composite began to lose significant weight at 180 °C, which is approximately 20 °C lower than that of sulfur, and presented a weight loss curve similar to that of sulfur below 285 °C. The low weight loss temperature was related to the fine hollow sulfur particles wrapped by PANI surface and was correspondingly observed in the DSC curves in Fig. 5b. Another significant difference was observed in Fig. 5b, where sulfur melting of polyaniline-wrapping hollow sulfur composite at 110 °C was significantly lower than that of sulfur particles at 120 °C. The low sulfur melting temperature stimulated sulfur diffusion through the heat generated in the charge/discharge cycles, which may have a potential effect on the electrochemical performance of polyaniline-wrapping hollow sulfur composite. Combined with the weight loss curve of PANI in Fig. 5a, the weight loss values of sulfur, PANI, and polyaniline-wrapping hollow sulfur composite were 100 wt%, 19.84 wt%, and 77.31 wt% at 320 °C, respectively. The sulfur content in the polyaniline-wrapping hollow sulfur composite was determined to be 71.69% through the following equation:

$$(Ms + Mp) \times 77.31\% = Ms \times 100\% + Mp \times 19.84\% \quad (2)$$

Ms: mass reaction of sulfur in composite material.
Mp: mass fraction of PANI in composite material.

3.2. Electrochemical performance

Fig. 6a and 6b show the cycle performance of sulfur and polyaniline-wrapping hollow sulfur composite. The charge and discharge capacities showed an increasing trend with increasing cycle time for sulfur and polyaniline-wrapping hollow sulfur composite. This trend was due to the activation caused by sulfur diffusion into the internal void space inside the polyaniline shell, wherein heat was generated and sulfur was melted during the charge/discharge process [14,15]. Thereafter, the charge and discharge capacities decreased when cycle time further increased. A difference was observed between sulfur and the polyaniline-wrapping hollow sulfur composite. The charge and discharge capacities of sulfur increased from its initial values of 326.7 and 268.5 mAh g^{-1} in the first cycle to the maximum values of 526 and

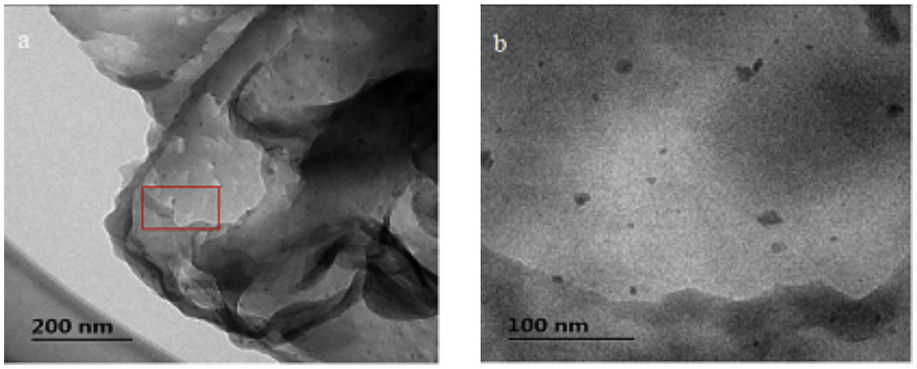

Fig. 4. TEM images of polyaniline wrapping hollow sulfur composite.

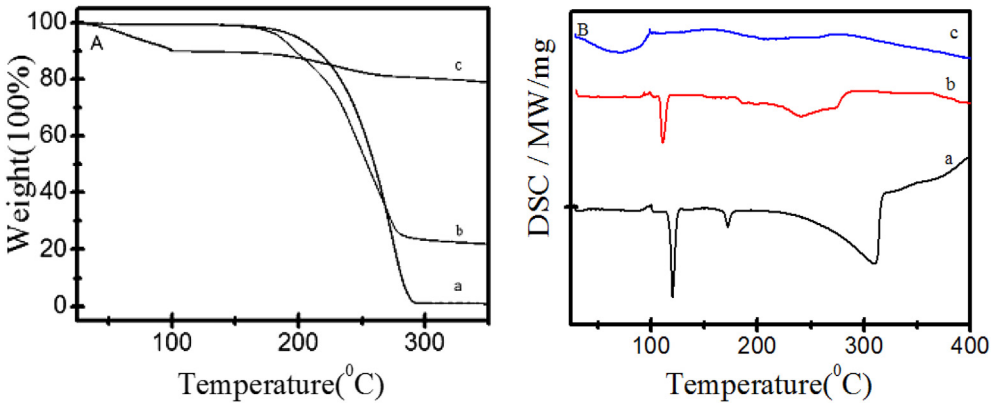

Fig. 5. TG (A) and DSC (B) curves of the sulfur (a), polyaniline wrapping hollow sulfur composite (b) and PANI(c).

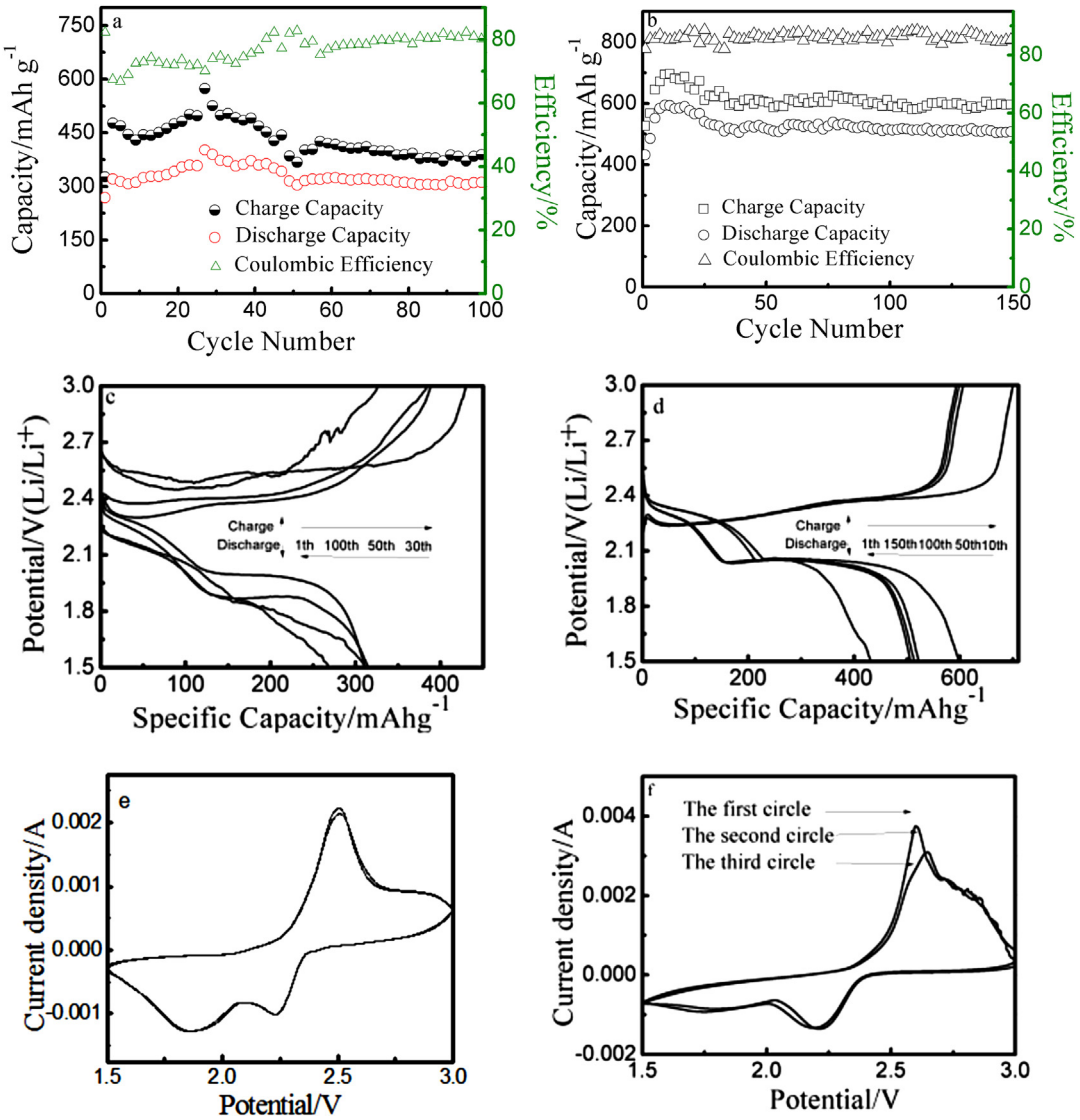

Fig. 6. Cycle performance (a, b), charge/discharge voltage curves (c, d) and cyclic voltammetry curves (e, f) of sulfur and polyaniline wrapping hollow sulfur composite.

384.1 mAh g^{-1} at the 30th cycle and then decreased irreversibly to 378 and 306.7 mAh g^{-1} at the 100th cycle. The charge and discharge capacities of the polyaniline-wrapping hollow sulfur composite increased from the initial values of 526 and 31.9 mAh g^{-1} in the first cycle to the maximum values of 700.6 and 598.4 mAh g^{-1} at the 10th cycle in the activation process, 606.7 and 522.9 mAh g^{-1} at the 50th cycle, 596.6 and 513.4 mAh g^{-1} at the 100th cycle, and 593.6 and 506.3 mAh g^{-1} at the 150th cycle. The charge and discharge capacities of the polyaniline-wrapping hollow sulfur composite presented stable values after a slight decrease following the activation process, in contrast to those of sulfur.

The detailed charge and discharge curves of sulfur and polyaniline-wrapping hollow sulfur composite are shown in Fig. 6c and 6d. The sulfur exhibited no platform in the first charge and discharge curves, which corresponded to the low charge and discharge capacities. At the 30th cycle, one charge platform and two discharge platforms were observed with the highest platform length and voltage. However, the platform length and voltage worsened at the 50th and 100th cycles, accompanied by the decreased charge and discharge capacities. In contrast to the charge and discharge curves of sulfur, those of polyaniline-wrapping hollow sulfur composite had one good charge platform and two discharge platforms in the first cycle. The charge and discharge platform voltages of polyaniline-wrapping hollow sulfur composite maintained stable values in the entire charge and discharge cycles. However, the charge and discharge platform lengths increased and then slightly decreased from the first to the 10th, 50th, 100th and 150th cycles. The improved electrochemical performance of the polyaniline-wrapping hollow sulfur composite was related to the oxidation–reduction of the cathode in the charge/discharge process.

Fig. 6e and 6f show the CV curves of lithium/sulfur cells tested with 0.2 mV s^{-1} scan rate. The sulfur cathode showed two significant cathodic peaks at 1.9 and 2.3 V as well as one anodic peak at 2.5 V [16]. The cathodic peaks corresponded to the formation of short polysulfides (S_6^{2-} and S_4^{2-}) by cyclooctasulfur (S8) reduction and the subsequent formation of insoluble lithium sulfide (Li_2S_2 or Li_2S) by short polysulfide reduction. In terms of the polyaniline-wrapping hollow sulfur cathode, the cathodic peak at 1.9 V became weak, and the peak at 2.3 V reduced slightly to 2.2 V, whereas the anodic peak at 2.50 V increased slightly to 2.64 V. The results reflected that the hollowed sulfur and its charge product

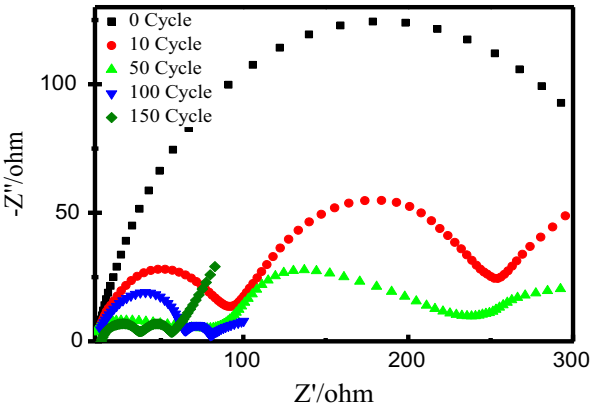

Fig. 7. Nyquist plots of polyaniline wrapping hollow sulfur composite at different cycle times.

Li_2S_2 (or Li_2S) wrapped by polyaniline was easily reduced and oxidized, respectively. This finding may be due to the fact that fine hollow sulfur wrapped polyaniline had significantly more electron conduction paths and thereby improved conductivity.

EIS was performed to demonstrate the cycle performance improvement of the polyaniline-wrapping hollow sulfur composite. Fig. 7 shows the typical Nyquist plots of the polyaniline-wrapping hollow sulfur composite at different charge and discharge cycles. The Nyquist plots had a large semicircle in the high frequency regions and an inclined line in the low-frequency regions before the charge and discharge cycles. The semicircle was divided into two small circles after the charge and discharge cycles. The semicircle at high frequency was considered as charge transfer resistances in the lithium–electrolyte interface, whereas the semicircle at medium frequency was likely associated with the charge transfer of lithium polysulfide intermediaries formed during the charge and discharge cycles [17]. According to the EIS results at the first, 10th, 50th, 100th, and 150th cycles, the semicircle greatly decreased as the process reached the 150th cycle, suggesting that the resistance successively reduced, and the formed lithium polysulfide intermediaries in the PANI films were attributed to a high conductivity for the charge transfer.

Here, the presented paper used chemical method to prepare high-performance polyaniline wrapping hollow sulfur composite. The improved electrochemical performance came from hollow nanometer sulfur wrapped by polyaniline. The flexible nanostructure enhanced conductivity of sulfur and provided a large void space, which accommodated sulfur expansion and prevented polysulfide dissolution during lithiation. Compared to the conventional co-heating of sulfur and polyaniline at high temperature [9,10], the chemical reactions including sulfur deposition and polyaniline wrapping occurred at room temperature and did not damage the polymer structure. The reactions could also be easily controlled to obtain fine hollow sulfur particle wrapped by polyaniline. The polyaniline wrapping hollow sulfur composite exhibited long stable cycling performance, which presented a promising future for large-scale Li-S batteries.

4. Conclusion

Polyaniline-wrapping hollow sulfur composite was prepared through in situ synthesis and was used to investigate the electrochemical properties of lithium/sulfur cells. The polyaniline-wrapping hollow sulfur composite presented an excellent reversible capacity of 506.3 mAh g^{-1} after 150 cycles at 0.1 C, which was significantly higher than that of sulfur at similar conditions. Microstructure and electrochemical results showed that the capacity increase was related to the following factors: increase of sulfur utilization because of a smaller sulfur particle size, enhancement of electrical contact, and decrease of active material loss because of sulfur and its charge product Li_2S_2 (or Li_2S) wrapped by polyaniline.

Acknowledgments

This work was financially supported by the Scientific Research Foundation for the Returned Scholars, postdoctoral support of P. R China (2015M581910), postdoctoral preferential support of Zhejiang province (BSH1502029), the National Science Foundation of China (Project No. 51501175), and the Guangxi Key Laboratory of Information Materials (Guilin University of Electronic Technology, project No. 1210908-02-K).

References

[1] J. Shim, K.A. Striebel, E.J. Cairns, The lithium/sulfur rechargeable cell, J. Electrochem. Soc. 149 (2002) a1321–a1325.
[2] S. Chen, X. Huang, H. Liu, 3D hyperbranched hollow carbon nanorod architectures for high-performance lithium-sulfur batteries, Adv. Energy Mater. 4 (8) (2014) 1301761.
[3] H. Yamin, E. Peled, Electrochemistry of a nonaqueous lithium/sulfur rechargeable cell, J. Power Sources 9 (1983) 281–287.
[4] Y.X. Yin, S. Xin, Y.G. Guo, L.J. Wan, Lithium-sulfur batteries: electrochemistry, materials, and prospects, Angew. Chem. Int. Ed. 52 (2013) 13186–13200.
[5] D. Bresser, S. Passerini, B. Scrosati, Recent process and remaining challenges in sulfur-based lithium secondary batteries-a review, Chem. Commun. 49 (2013) 10545–10562.
[6] W.D. Zhou, Y.C. Yu, H. Chen, F.J. Disalvo, H.D. Abruna, Yolk-shell structure of polyaniline-coated sulfur for thium-sulfur batteries, J. Am. Chem. Soc. 135 (44) (2013) 16736–16743.
[7] W.Y. Li, Q.F. Zhang, G.Y. Zheng, Z.W. She, H.B. Yao, Y. Cui, Understanding the role of different conductive polymers in improving the nanostructure sulfur cathode performance, Nano Lett. 13 (11) (2013) 5534–5540.
[8] L. Wang, J. Chen, K. Konstantinov, L. Zhao, S.H. Ng, G.X. Wang, Z.P. Guo, H.K. Liu, Sulphur-polypyrrole composite positive electrode materials for rechargeable lithium batteries, Electrochem. Acta 51 (22) (2006) 4634–4638.
[9] L.L. Qiu, S.C. Zhang, L. Zhang, M.M. Sun, W.K. Wang, Preparation and enhanced electrochemical properties of nano-sulfur/poly (pyrrole-aniline) cathode material for lithium/sulfur batteries, Electrochem. Acta 55 (2010) 4632–4636.
[10] L. Xiao, Y. Cao, B. Schwenzer, M.H. Engelhard, L.V. Saraf, Z. Nie, G.J. Exarhos, J. Liu, A soft approach to encapsulate sulfur: polyaniline nanotubes for lithium-sulfur batteries with long cycle life, Adv. Mater. 24 (2012) 1176–1181.
[11] G.Q. Ma, Z.Y. Wen, J. Jin, Y. Lu, X.W. Wu, M.F. Wu, C.H. Chen, Hollow polyaniline sphere@sulfur composites for prolonged cycling stability of lithium-sulfur batteries, J. Mater. Chem. A 2 (2014) 10350–10354.
[12] M.Q. Wang, W.K. Wang, A.B. Wang, K.Q. Yuan, L.M. Miao, X.L. Zhang, Y.Q. Huang, Z.B. Yu, J.Q. Qiu, A multi-core-shell structured composite cathode material with a conductive polymer network for Li-S batteries, Chem. Commun. 49 (2013) 10263–10265.
[13] P. Wei, M.Q. Fan, H.C. Chen, X.R. Yang, H.M. Wu, J.D. Chen, T. Li, L.W. Zeng, Y.J. Zou, High-capacity grapheme/sulfur/polyaniline ternary composite cathode with stable cycling performance, Electrochem. Acta 174 (2015) 963–969.
[14] H.S. Ryu, H.J. Ahn, K.W. Kim, J.H. Ahn, J.Y. Lee, Discharge process of Li/PVdF/S cells at room temperature, J. Power Sources 153 (2006) 360–364.
[15] D.W. Wang, Q.C. Zeng, G.M. Zhou, L.C. Yin, F. Li, H.M. Cheng, I.R. Gentle, Carbon-sulfur composites for Li-S batteries: status and prospects, J. Mater. Chem. 1 (2013) 9382–9394.
[16] Y.J. Choi, Y.D. Chung, C.Y. Baek, K.W. Kim, Effects of carbon coating on the electrochemical properties of sulfur cathode for lithium/sulfur cell, J. Power Sources 184 (2008) 548–552.
[17] A. Konarov, D. Gosselink, T.N.L. Doan, Y.G. Zhang, P. Chen, Simple, scalable, and economical preparation of sulfur–PANI composite cathode for Li/S batteries, J. Power Sources 259 (2014) 183–187.